J Therm Anal Calorim (2010) 102:557–562
DOI 10.1007/s10973-010-0978-3

Predicting the shock sensitivity of cyclotrimethylene-trinitramine

Victor J. Bellitto · Mikhail I. Melnik · Daniel N. Sorensen · Joseph C. Chang

NATAS2009 Special Issue

Abstract We studied the surface and thermal properties of seven different varieties of cyclotrimethylene-trinitramine (RDX) crystalline explosives from five manufacturers using differential scanning calorimetry (DSC) and atomic force microscopy (AFM). The specific varieties of the RDX studied were acquired from the previous Reduced Sensitivity RDX Round Robin program. They were chosen because intensive characterization of the materials already existed including shock sensitivity and cyclotetramethylene-tetranitramine (HMX) impurity levels. AFM scans revealed a diversity of surface defects. To quantify the surface defects on the crystalline surface of the RDX particles, surface roughness measurements were acquired. Statistical analysis was undertaken to correlate the observed surface, HMX impurity levels, and DSC thermal curve properties with the known shock sensitivities of the material. It was determined that a statistically significant relationship exists between surface roughness and the shock sensitivity of the material while no relationship was observed between the DSC thermal properties and either surface roughness or shock sensitivity. The HMX content greatly affected the thermal properties of RDX but was uncorrelated with the shock sensitivity.

Keywords RDX · HMX · Statistical · DSC · AFM · Surface

V. J. Bellitto (✉) · D. N. Sorensen · J. C. Chang
Naval Surface Warfare Center, 4104 Evans Way, Suite 102, Indian Head, MD 20640-5102, USA
e-mail: victor.bellitto@navy.mil

M. I. Melnik
Department of Commerce, Niagara University, PO Box 2201, Niagara, NY 14109-2201, USA

Introduction

There is considerable interest in the development of explosives and propellants that are insensitive to shock or friction. Insensitive munitions have the potential to reduce the hazards of munitions storage and transport as well as the potential to increase storage and transport capabilities. Cyclotrimethylene-trinitramine (RDX), a widely used high-explosive, has been the focus of much research interested in obtaining a relationship between its crystalline properties and its shock sensitivity. The interest culminated with the formation of the Reduced-Sensitivity RDX Round Robin program, an international inter-laboratory comparison investigation [1]. Initial studies have shown that particle size [2], density [3, 4], and crystal morphology [5] play a role in the shock sensitivity of RDX. Recently it has been reported that surface properties of the RDX particles contribute to its sensitivity. Analysis performed using atomic force microscopy (AFM) have related surface roughness parameters of RDX particles with its shock sensitivity [6, 7]. Studies using scanning electron microscopy and porosimetry have reported that 10–30 μm RDX particles with a greater surface roughness were more shock-sensitive [8]. It has also been reported that differential scanning calorimetry (DSC) could be a useful method to differentiate between RDX materials having different shock sensitivities [9, 10].

In this investigation DSC, AFM, and advanced statistical analysis were conducted to examine the relationship between the surface and thermal properties of the RDX crystalline powders and their effect on the shock sensitivity of the crystalline high explosive. We studied seven varieties of RDX with previously characterized properties such as impurity level, methods of manufacture, and shock sensitivity. The specific varieties of the RDX materials studied were acquired from the previous Reduced

Sensitivity RDX Round Robin program [1]. The two methods for the manufacture of RDX are Type I) produced by direct nitration known as the Woolwich process and Type II) produced by the acetic anhydride method known as the Bachman process. Vendor proprietary treatments are also performed on some samples to reduce sensitivity. The major impurity in RDX is cyclotetramethylene-tetranitramine (HMX) and has been reported to be as high as 17% [1]. The measure of shock sensitivity, determined through a large-scale gap test, is the relative shock intensity required to produce detonation of the test sample 50% of the time. The shock wave from the initiating charge before entering the test sample is attenuated by varied card thicknesses of poly(methylmethacrylate) (PMMA). The shock pressure entering the sample is determined from calibrations of the initiating charge-attenuating thickness system. A larger number of cards measured to achieve the 50% detonation translates to a smaller shock wave entering the sample and thus a more shock-sensitive sample.

Experimental method

The RDX powders and formulations used in testing were part of a larger study characterizing the observable differences between RDX types [1]. The only difference in formulation manufacture was the type/class of RDX used. Sample formulations were kept in temperature-controlled magazines until testing. From other testing no moisture effect was anticipated in these samples. Samples were prepared under the same conditions so that the only observable differences would be due the variety of RDX studied. The test samples for the DSC analysis and the large-scale gap test were prepared as a polymer-bonded explosive composition of 64% RDX, 20% aluminum, and 16% hydroxy-terminated polybutadiene (HTPB) binder [1].

Differential Scanning Calorimetry was performed on a TA Instruments Model Q1000 after calibration against indium and zinc extrapolated melt onsets as temperature standards. Indium was also used as the heat flow standard. The heating rate used for both calibration and testing was 5 °C min^{-1}. Each sample was prepared in TA Instruments' traditional style hermetic aluminum pans under normal laboratory temperature and atmospheric conditions. The sample masses tested were between 0.5 and 0.6 mg of each formulation as measured on a balance reading to five decimal places. This mass range allowed for decomposition without concern for thermal runaway. Testing was performed under 50 mL min^{-1} nitrogen purge. All data were reported in terms of W g^{-1} of the formulation. The curve characteristics chosen for study were the extrapolated melt onset, the melt minima, the extrapolated decomposition onset, and the peak decomposition temperature. While it is recognized that the extrapolated melt onset is the recognized DSC melting point, the melt minima is relevant in that RDX melts with decomposition. The minima peak position differences with respect to heat transfer should be small in that similar masses were used for testing and the only difference between these formulations is the variety of RDX used as the oxidizer.

Atomic force microscopy was used to study the surface properties of the RDX high explosive crystals. The AFM analysis was performed using a Multimode V scanning probe microscope (Veeco Instruments). The instrument was operated in Tapping Mode, where topographical analysis is performed with minimal contact of the surface. It maps topography by lightly tapping the surface with an oscillating probe tip. The cantilever's oscillation amplitude changes with sample surface topography, and the topography image is obtained by monitoring these changes and closing the z feedback loop to minimize them.

A variety of surface defects were observed including edge and screw dislocations, voids, cracks, etc. An example of a topographical image obtained by AFM of the RDX particle surface is shown in Fig. 1a and its amplitude image is shown in Fig. 1b. The amplitude image is equivalent to a map of the slope of the sample; it often displays the shape of the sample more easily. The z-scale in amplitude shows the tip deflection as it encountered sample topography. The amplitude image on harder samples, highlights the edges of features, and on softer samples, can depict subsurface features better than the topography image.

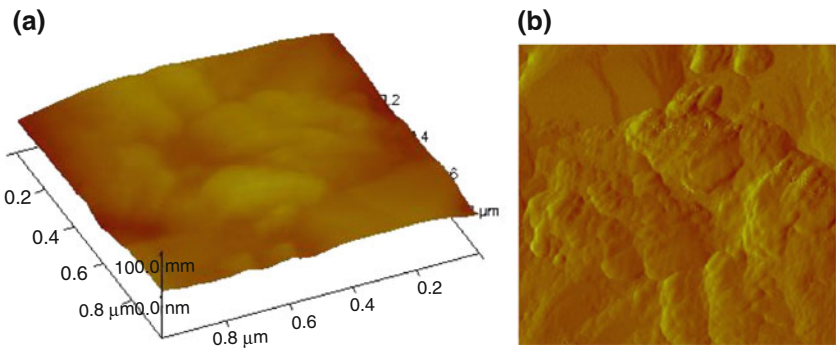

Fig. 1 AFM image of an RDX particle surface showing **a** surface topography and **b** acquired as an amplitude image

Since the defects affect the crystallinity of the material and thus affect the surface roughness, the root mean square (RMS) of the surface topography was used to gauge the roughness. The surface morphological images acquired in height mode were quantitatively compared using the RMS roughness calculation (R). The roughness was determined by finding the median surface height for the image and then evaluating the standard deviation of the image. The equation for calculating the surface roughness is

$$R = \sqrt{\frac{1}{MN}\sum_{k=0}^{M-1}\sum_{l=0}^{N-1}\left[z(x_k, y_l) - \mu\right]^2},$$

where μ is the mean value of the height, z, across all in-plane coordinates (x, y):

$$\mu = \frac{1}{MN}\sum_{k=0}^{M-1}\sum_{l=0}^{N-1} z(x_k, y_l).$$

Results and Discussion

A basic summary of the seven materials used in our study is presented in Table 1. The samples exhibit significant variation in terms of their levels of HMX concentration, shock sensitivity, DSC thermal properties, and mean surface roughness (R_m) as measured by our laboratory. To investigate the surface characteristics, multiple scans on several particles for each of the materials were obtained. An average of 5–6 scans were acquired per particle, and five particles for each material were analyzed, resulting in the acquisition of 190 scans. The multiple 1-μm scans of each particle surface provide a distribution of R (RMS) for each particle. The surface roughness is quantified for each particle (p) and material (m), and the average measure of roughness $\bar{R}_{pm}$ is computed. Averaging these for each material provides the average value of the distribution of the mean,

$$R_m = \frac{1}{N}\sum_{p} \bar{R}_{pm},$$

an unbiased estimator for the average measure of surface roughness of material m.

The comparative overlays of the DSC data are shown in Fig. 2a and b. While the decomposition peaks are within 2.1 °C of one another showing agreement within the anticipated precision of the instrument, the endothermic activity shows more deviation. Materials A and D are shown separately in Fig. 2b as they display lower endotherms relative to the other samples. These early endotherms are consistent with reported HMX containing RDX with the melt occurring in the 188–205 °C range [1, 10, 11].

The correlation coefficients between the main variables of interest used in our analysis are presented in Table 2. The thermal characteristics of the RDX materials appear to be strongly correlated with the level of HMX concentration. Higher levels of impurity, as represented by higher presence of HMX in the RDX structure, are strongly positively correlated with the decomposition maximum temperature and strongly negatively correlated with the melting minimum temperature. The latter is an anticipated colligative property. We also note a relatively high negative correlation between the melting minimum temperature and the decomposition maximum temperature (−0.670). However, neither of the thermal variables appears to be correlated with the shock sensitivity in these RDX materials. Furthermore, the level of HMX impurity also appears to be uncorrelated with the shock sensitivity. However, the surface roughness measure (R_m) does seem to be strongly negatively correlated with the measure of shock sensitivity.

Table 1 Summary statistics for the seven RDX samples

Manufacturer	Ordnance Systems Inc.	Eurenco	Eurenco	Dyno Nobel	Dyno Nobel	ADI	Royal Ordnance Defense
Grade	RDX	I-RDX	MI-RDX	Type II	RS-RDX	Grade A	Grade A
Type	II	I	I	II	II	I	I
Mean % HMX	7.36	0.02	0.03	8.55	0.82	0.02	0.19
SD (Mean % HMX)	0.92	0.08	0.02	2.28	0.10	0.01	0.13
Shock sensitivity/GPa	4.2	4.66	2.21	3.86	5.24	5.21	5.06
Melt minima/°C	200	204.82	204.24	194.87	204.87	204.81	204.97
Decomposition peak/°C	227.87	226.17	226.48	227.31	226.94	225.73	226.61
Extrapolated melt onset/°C	197.87	203.21	203.56	187.01	204.67	203.46	203.83
Extrapolated decomp. onset/°C	216.86	220.47	221.77	219.56	218.28	222.98	219.81
R_m (mean surface roughness)/nm	18.27	8.43	16.04	10.56	5.32	10.07	6.15
SD (R_m)	4.13	4.85	11.03	9.81	3.62	3.61	2.88

The mean % HMX, SD (mean % HMX), and shock sensitivity values are obtained from Ref. [1]

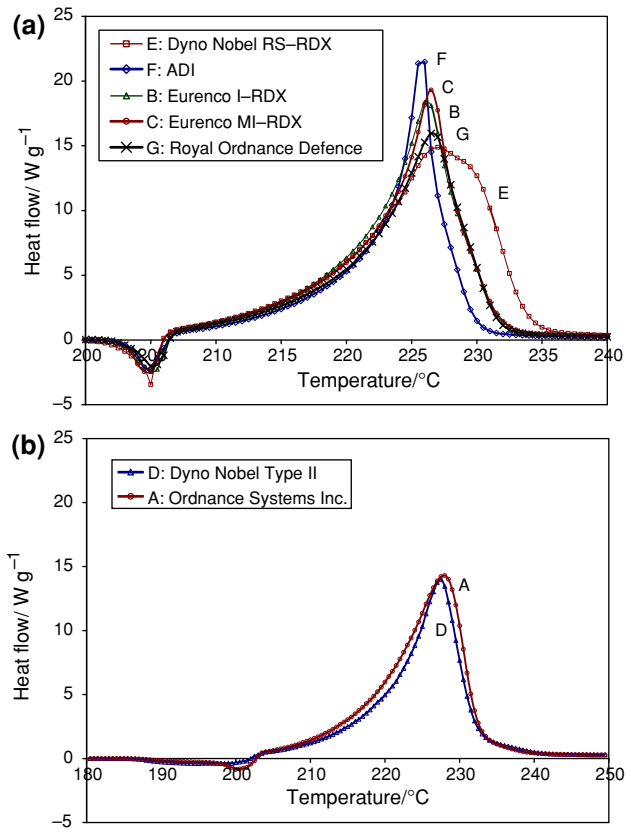

Fig. 2 **a** DSC thermographs of five RDX samples having lower HMX impurity (Exothermic reaction in the sample is shown as positive heat flow) **b** DSC thermographs of two RDX samples having higher HMX impurity (Exothermic reaction in the sample is shown as positive heat flow)

To further investigate these relationships we employ a standard regression analysis technique, OLS (Ordinary Least Squares) [12]. This technique enables the capture of the statistical relationships between these variables. The first sets of reported estimations from the regression analysis are shown in Table 3.

The numbers displayed in parenthesis in Tables 3, 4, and 5 represent the standard error of the coefficient above the parenthesis. A large error relative to the magnitude of the coefficient suggests a lack of statistical significance of the coefficient. For the ease of reading, the statistically significant coefficients are identified with asterisks.

The results demonstrate that the thermal characteristics of the RDX materials tend to be largely determined by the HMX impurity concentration. The exception is the extrapolated decomposition onset temperature, where the coefficient on the mean % HMX is only marginally statistically significant at 84% confidence level. Our results suggest that the variability in the melting temperature of RDX materials can be almost entirely explained by the level of impurity. The adjusted R^2 measure suggests that nearly 88% of this variability is driven by the HMX concentration.

The decomposition peak temperature is also affected by the level of impurity (Specification II). Interestingly, the effect is positive, higher impurity increases the decomposition temperature. However, impurity alone only explains about 62% of the variability in the decomposition peak temperature, and the effect on the temperature is relatively small.

The temperature range between the melting minima and the decomposition peak temperatures (Specification III) is almost completely explained by the level of impurity, which accounts for 93.5% of the fluctuation in the temperature range.

Two additional specifications are presented in Table 4. Specification I examines the impact impurity has on the difference between the melting and extrapolated melting onset temperatures, while specification II does the same for the difference between the decomposition and extrapolated decomposition onset temperatures. The goodness of fit of these models is considerably weaker, but impurity continues to play a statistically significant role in Specification I. Higher impurity values increase the gap between the extrapolated melting onset and the melting minima temperatures.

As a colligative property, impurity is a key factor in explaining the melting temperature of the RDX materials. Since Type I production of RDX, without further processing, results in significantly lower levels of HMX impurity, type of production, and its relationship to shock sensitivity are examined in Table 5. The specification uses

Table 2 Correlation coefficients between thermal characteristics, impurity, shock sensitivity, and surface roughness of RDX

	Mean % HMX	Shock sensitivity	Melt minima temp.	Decomposition peak temp.	R_m
Mean % HMX	1				
Shock sensitivity	−0.181	1			
Melt minima temp.	−0.949	0.278	1		
Decomposition peak temp.	0.825	−0.184	−0.670	1	
R_m	0.448	−0.694	−0.349	0.410	1

Table 3 Regression analysis of thermal characteristics I

Specification	Dep. Var.				
	DSC melt minima temp. I	DSC decomp. peak temp. II	DSC temp. (decomp.-melt) III	Melt onset temp. IV	Decomp. onset temp. V
Mean % HMX	−0.965*** (0.144)	0.155** (0.048)	1.120*** (0.120)	−1.507*** (0.325)	−0.318 (0.195)
Constant	204.996*** (0.616)	226.353*** (0.203)	21.357*** (0.513)	204.173*** (1.391)	220.732*** (0.835)
Adj R^2	0.8797	0.6162	0.9349	0.773	0.215

*** 99% statistical significance and higher

** 95% statistical significance and higher

* 90% statistical significance and higher

Table 4 Regression analysis of thermal characteristics II

	Melt minima temp.–Melt onset temp.	Decomp. peak temp.–decomp. onset temp.
Specification	**I**	**II**
Mean % HMX	0.542** (0.186)	0.473 (0.239)
Constant	0.823 (0.796)	5.621*** (1.020)
Adj R^2	0.5544	0.3278

See Table 3 footer

a binary variable that assumes the value of 1 if Type 1 process is used, and zero otherwise. Shown in Table 5 are the estimations where the dependent variable is the shock sensitivity. We note that the HMX impurity does not appear to have any statistically significant impact on the measure of shock sensitivity (Specification I). This is in agreement with HPLC analysis performed by Borne and Ritter [13], which found no correlation between HMX content and shock sensitivity of RDX-based cast explosives. Although the authors also claim that HMX content in excess of 1% leads to shock-sensitive formulations while formulations with HMX contents of less than 0.15% no correlation was observed. Contrary results have been reported by Oxley et al. [10] who observed a correlation between increased HMX content and increased sensitivity. The results in Table 5 also suggest that the type of production used (Specification II) and the thermal characteristics (Specifications III and IV) produce no statistically significant impact on the shock-sensitivity measure. We also regressed the shock sensitivity on the extrapolated melt onset and extrapolated decomposition onset temperatures, the results were similar to the reported Specification II and III results, as neither extrapolated melt onset nor extrapolated decomposition onset produced any statistically significant effects. Specification IV includes the R_m (mean surface roughness). We find that the surface roughness measure alone is responsible for explaining 38% of the variation in the sensitivity of the RDX materials. The coefficient suggests that a 1-point increase in the roughness measure reduces the sensitivity by 0.154.

Separately, we investigated the impact the mean surface roughness (R_m) has on the melt minima temperature and the decomposition peak temperature of the RDX. Our empirical study found no statistical relation between R_m and the melt and decomposition temperatures. The adjusted R^2 remained less than 0.002 in the regression where the melting temperature and the decomposition temperature

Table 5 Regression analysis of shock sensitivity

Specification	Sensitivity I	Sensitivity II	Sensitivity III	Sensitivity IV
Mean % HMX	−0.051 (0.125)			
Type I production		−0.148 (0.900)		
DSC melt minima temp.			0.078 (0.180)	
DSC decomp. peak temp.			0.0059255 (0.975)	
R_m				−0.154* (0.072)
Constant	4.473*** (0.533)	4.433*** (0.680)	−12.858 (246.932)	5.998*** (0.830)
Adj R^2	−0.161	−0.194	−0.384	0.378

See Table 3 footer

Adjusted R^2 is computed using the following formulation: $1 - ((1 - R^2)((N - 1)/(N - K - 1)))$ where N is the number of observations and K is the number of independent variables. Adjuster R^2 values can be negative indicating that the independent variables fail to explain the variations in the dependent variable

were separately regressed on the mean surface roughness. It appears that the thermal properties of these RDX formulations are unaffected by the surface roughness characteristics of the RDX particles.

It is important to note that our statistical analysis is limited to seven materials, which increases the impact each observation (material) has on our regression coefficients.

Conclusions

Defects inherent within crystalline RDX should be observable on the surface using AFM since defects cause the periodicity of the crystal to be disturbed over several atomic layers. But our results demonstrate that there is no statistical relationship between the HMX impurity and the surface roughness or shock sensitivity of the material. The AFM data provide evidence that the HMX impurity is not the major factor affecting the shock sensitivity of RDX. The DSC results demonstrate that the HMX impurity is a key factor in explaining the characteristic observed in the thermal curves while no relationship was observed between the DSC thermal properties and either surface roughness or shock sensitivity of RDX.

Acknowledgements This study was supported by the Office of Naval Research (ONR) and the Naval Surface Warfare Center (NSWC) at Indian Head, MD. The authors are grateful to Dan Simons, Paul Conolly, Lt. Col. Ries and Cliff Anderson for their support of this research at ONR. The authors also gratefully acknowledge Gerry Pangilinan, Dorothy Cichra, and Tom Russell for their support at NSWC. The authors express their thanks to Mary Sherlock, Robert Raines, Tina Woodland, and Philip Thomas for helpful discussions and for providing the samples.

References

1. Doherty RM, Watts DS. Relationship between RDX properties and sensitivity. Propellants Explos Pyrotech. 2008;33:4–13.
2. Moudard H, Kury JW, Delclos A. The effect of particle size on the shock sensitivity of cast PBX formulations. In: Proceedings of the 8th Symposium (International) on Detonation, Albuquerque, NM, 1985.
3. Borne L. Influence of intragranular cavities of RDX particle batches on the sensitivity of cast wax bonded explosives. In: Proceedings of the 11th Symposium (International) on Detonation, Boston, MA, 1993.
4. Baillou F, Dartyge JM, Spyckerelle C, Mala J. Infuence of crystal defects on sensitivity of explosives. In: Proceedings of the 10th Symposium (International) on Detonation, Boston, MA, 1993.
5. van der Steen AC, Verbeek HJ, Meulenbrugge JJ. Influence of RDX crystal shape on the shock sensitivity of PBXs. In: Proceedings of the 9th Symposium (International) on Detonation, Portland, Oregon, 1989.
6. Lecume S, Spyckerelle, Sommer F. Structure of pristine crystal defects revealed by AFM and Microtomography. In: Shock Compression of Condensed Matter-2003. New York: American Institute of Physics; 2004. pp. 997–1000.
7. Bellitto VJ, Melnik MI. Surface defects and their role in the shock sensitivity of cyclotrimethylene-trinitramine. Appl Surf Sci. 2010;256:3478–81.
8. Czerski H, Proud WG. Relationship between the morphology of granular HMX and its shock sensitivity. J Appl Phys. 2007;102:113515–8.
9. Spyckerelle C, Freche A, Eck G. Aging of reduced sensitivity RDX and compositions based on reduced sensitivity RDX, an update. In: Proceedings of the 2006 Insensitive Munitions and Energetic Materials Technology Symposium, Bristol, UK, 24–28 April 2006.
10. Oxley J, Smith J, Buco R, Huang J. A study of reduced-sensitivity RDX. J Energy Mater. 2007;25:141–60.
11. McKenney RL Jr, Krawietz TR. Binary phase diagram. Series: HMX/RDX. J Energy Mater. 2003;21:141–66.
12. Greene WH. Econometric Analysis. 5th ed. Upper Saddle River, NJ: Prentice Hall; 2003.
13. Borne L, Ritter H. HMX as an impurity in RDX particles: effect on the shock sensitivity of formulations based on RDX. Propellants Explos Pyrotech. 2006;31:482–9.